International Journal of Ocean System Engineering 1(3) (2011) 136-143
http://dx.doi.org/10.5574/IJOSE.2011.1.3.136

Numerical Simulation of 3D Free-Surface Flows by Using CIP-based and FV-based Methods†

Kyung-Kyu Yang[1], Bo-Woo Nam[1,2] and Yonghwan Kim[1*]

[1]*Department of Naval Architecture and Ocean Engineering, Seoul National University, Seoul, Korea*

[2]*Maritime and Ocean Engineering Research Institute, KORDI, Daejeon, Korea*

(Manuscript Received June 1, 2010; Revised July 2, 2011; Accepted July 29, 2011)

Abstract

In this paper, three-dimensional free-surface flows are simulated by using two different numerical methods, the constrained interpolation profile (CIP)-based and finite volume (FV)-based methods. In the CIP-based method, the governing equations are solved on stationary staggered Cartesian grids by a finite difference method, and an immersed boundary technique is applied to deal with wave-body interactions. In the FV–based method, the governing equations are solved by applying collocated finite volume discretization, and body-fitted meshes are used. A free-surface boundary is considered as the interface of the multi-phase flow with air and water, and a volume-of-fluid (VOF) approach is applied to trace the free surface. Among many variations of the VOF-type method, the tangent of hyperbola for interface capturing (THINC) and the compressive interface capturing scheme for arbitrary meshes (CICSAM) techniques are used in the CIP-based method and FV-based method, respectively. Numerical simulations have been carried out for dam-breaking and wave-body interaction problems. The computational results of the two methods are compared with experimental data and their differences are observed.

Keywords: Wave-body interaction, CIP, FVM, VOF, THINC, CICSAM

1. Introduction

Wave-body interaction problems are important for the design of ships and offshore structures. Potential-based codes give reasonable results for engineering purposes. However, they have some limitations in simulating strongly nonlinear wave-body interaction flows. Among alternative approaches, direct numerical methods based on the Navier-Stokes or Euler equations are becoming popular, due to the dramatic increase of computational resources. Yang and Löehner [1] also demonstrated highly nonlinear wave-body interaction simulations such as slamming and green water using VOF and FEM, and suggested an efficient extrapolation algorithm. Hu et al. [2] demonstrated some three-dimensional computations of strongly nonlinear wave-ship interaction problems by using the CIP method. Monroy et al. [3] presented the Reynolds Averaged Navier-Stokes (RANS) simulations of ship motions in regular and irregular head seas, cooperating with potential-based incident waves.

The major difficulty in the numerical simulation of highly nonlinear wave-body problems is that the topology of the free-surface boundary can be largely distorted, fragmented and merged. The volume-of-fluid method is one of the most popular schemes for studying two-phase flow problems with a free surface. In the VOF method, computations can be performed on a fixed grid system without an interface tracking procedure, and the interface is captured as part of the solution while ensuring mass conservation. Among many variations of the VOF method, CICSAM, which was first suggested by

†This paper was presented at the PACOMS 2010 conference, Busan, Korea, November 2010.

*Corresponding author. Tel.: +82-2-880-1543, Fax.: +82-2-876-9226.
E-mail address: yhwankim @snu.ac.kr.

Ubbink and Issa [4], is adopted for the FV-based method, because this method is flexible enough to apply an unstructured grid system and to appropriately retain the transitional region between the two fluids during the long-time simulations. Recently, Xiao et al. [5] developed the tangent of hyperbola for interface capturing (THINC) scheme, showing good performance compared with the other interface capturing methods, even when compared with a very simple algorithm. This method is adapted for the CIP-based method. In this paper, a mathematical model is based on the three-dimensional unsteady incompressible Navier-Stokes equation which is solved by two different numerical methods, the CIP and FV based methods. In the CIP-based method, the Navier-Stokes equation is solved on a stationary staggered Cartesian grid by a finite difference method, and the immersed boundary technique is applied to deal with wave-body interactions. In the FV–based method, the governing equations are solved by using collocated finite volume discretization, and body-fitted meshes are used. To compare and verify the accuracy of the developed methods, numerical simulations have been carried out for two problems: a dam-breaking problem with an obstacle, and a wave-body interaction for a truncated circular cylinder.

2. Numerical methods I: CIP-based method

2.1 Field equation solver

The CIP method was developed by Takewaki [6] in order to reduce numerical diffusion. The key idea of the CIP method is to approximate both a physical parameter, say *f*, and its spatial derivatives as cubic polynomials at grid points for the interpolation of parameters inside a cell. Once the interpolation function is constructed, a semi-Lagrangian procedure is applied for time evolution as follows:

$$f^{n+1}(\mathbf{x}) = f^{n}(\mathbf{x}-\mathbf{u}\Delta t); g^{n+1}(\mathbf{x}) = g^{n}(\mathbf{x}-\mathbf{u}\Delta t) \tag{1}$$

where $g = \partial f / \partial x_i$, $(i = 1,2,3)$.

The flow solver is the CIP-combined unified procedure (CCUP) method (Yabe [7]) based on the fractional step method and the CIP scheme for advection equations. The governing equations to be considered are as follows:

$$\frac{\partial u_i}{\partial x_i} = 0 \tag{2}$$

$$\frac{\partial u_i}{\partial t} + u_j \frac{\partial u_i}{\partial x_j} = -\frac{1}{\rho}\frac{\partial p}{\partial x_i} + \frac{1}{\rho}\frac{\partial}{\partial x_j}\left(\mu \frac{\partial u_i}{\partial x_j}\right) + f_i^b \tag{3}$$

$$\frac{\partial\left(\partial_\xi u_i\right)}{\partial t} + u_j \frac{\partial\left(\partial_\xi u_i\right)}{\partial x_j} = -\left(\partial_\xi u_j\right)\frac{\partial u_i}{\partial x_j} - \frac{\partial}{\partial \xi}\left(\frac{1}{\rho}\frac{\partial p}{\partial x_i}\right) + \frac{\partial S_i}{\partial \xi} \tag{4}$$

where $\xi = x_i$, $i = 1,2,3$ and S_i is a source term except for the pressure gradient term. f_i^b is an external body force. The time evolutions in Eqs. (3) and (4) are performed by a fractional step method, that is, a solving procedure is divided into three steps: one advection phase and two non-advection phases. At the first step, we solve the equation with only an advection terms by the CIP or rational CIP (RCIP) methods. Instead of using a cubic-polynomial interpolation function in the conventional CIP method, the RCIP method uses a rational function as follows:

$$f_i^{n+1} = F_i(x_i - u\Delta t),\ F_i(x) = \frac{\sum_{0\le l_x\le 3} C_{l_x}\left(x-x_i\right)^{l_x}}{\sum_{0\le p\le 1}\alpha_p\beta_p\left(x-x_i\right)^{p}} \tag{5}$$

The coefficients can be uniquely determined by using function values and the gradient values at each cell boundary. For multi-dimensional cases, the details can be found in Xiao et al. [8].

In the second step, the equations with diffusion and external force terms are solved by an explicit Euler algorithm. Finally, the pressure Poisson equation is solved by an iterative scheme to satisfy Eq. (2). The Poisson equation for pressure can be written as follows:

$$\nabla\cdot\left(\frac{1}{\rho}\nabla p^{n+1}\right) = \frac{1}{\Delta t}\nabla\cdot\mathbf{u}^{**} \tag{6}$$

Here, the superscript n+1 denotes the quantities at the next time step, and the double asterisk denotes the intermediate values obtained after the non-advection phase. After the pressure is obtained in the divergence-free velocity field, the velocity components are updated. The time step is then advanced to the next time step.

2.2 Free-surface capturing method

The free surface is determined by an interface capturing method. To identify the different phases in the multi-phase flow, a density function ϕ_m is defined for liquid (m=1), gas (m=2), and solid body (m=3). The density function for the liquid phase ϕ_1 is calculated by solving the following advection equation:

$$\frac{\partial \phi_1}{\partial t} + u_i \frac{\partial \phi_1}{\partial x_i} = 0 \tag{7}$$

The density function for the gas phase ϕ_2 can then be calculated from a simple constraint $\sum_m \phi_m = 1$ for each cell.

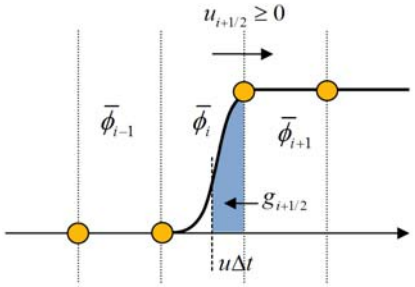

Fig. 1. Concepts of THINC method $u_{i+1/2} \geq 0$

The THINC scheme introduced by Xiao et al. [5] is used in the present computation. In this scheme, the profile of the density function inside a cell is approximated with hyperbolic tangent function to reproduce the jump of the density function near the free surface. As shown in Fig. 1, the THINC method uses the cell-averaged density function ($\bar{\phi}$) with temporal integration which is updated from the following equation:

$$\bar{\phi}_i^{n+1} = \bar{\phi}_i^n + \frac{1}{\Delta x_i}\left(g_{i-\frac{1}{2}} - g_{i+\frac{1}{2}}\right) + \frac{\Delta t}{\Delta x_i}\bar{\phi}_i^n\left(u_{i+\frac{1}{2}} - u_{i-\frac{1}{2}}\right) \tag{8}$$

where $\Delta x_i = x_{i+1/2} - x_{i-1/2}$, $\Delta t = t^{n+1} - t^n$. $g_{i+1/2}$ refers numerical flux through the cell boundary, which is defined as $g_{i+1/2} = \int_{t^n}^{t^{n+1}} (u\phi)_{i+1/2} dt$. The numerical fluxes are calculated by a semi-Lagrangian method similar to the CIP scheme, but the THINC scheme uses a tangent hyperbolic function, instead of using a polynomial, as follows:

$$F_i(x) = \frac{\alpha}{2}\left\{1 + \gamma \tanh\left[\beta\left(\frac{x - x_{i-1/2}}{\Delta x_i}\right) - \delta\right]\right\} \tag{9}$$

where α determines the maximum value of the interpolation function, β is related to the steepness of the jump, fixed as 3.5 in this computation, γ is determined according to the slope orientation of the jump, and δ is calculated by solving the following equation:

$$\frac{1}{\Delta x_i}\int_{x_{i-1/2}}^{x_{i+1/2}} F_i(x)\,dx = \bar{\phi}_i^n \tag{10}$$

Multi-dimensional computation is performed by operator splitting. The details can be found in Xiao [5].

3. Numerical methods II: FV-based method

The governing equations in the fluid domain are the continuity and incompressible Euler equations, which are written in conservative forms as follows (Ferziger and Peric [9]):

$$\frac{\partial}{\partial t}\int_\Omega \rho d\Omega + \int_S \rho u_j n_j dS = 0 \tag{11}$$

$$\frac{\partial}{\partial t}\int_\Omega \rho u_i d\Omega + \int_S \rho u_i u_j n_j dS = \int_\Omega \left(\frac{\partial \tau_{ij}}{\partial x_j} - \frac{\partial p}{\partial x_i} + \rho b_i\right) d\Omega \tag{12}$$

Here, Ω denotes the control volume and S is the control surface enclosing Ω. ρ and p are the fluid density and pressure, respectively. x_i is the Cartesian coordinate vector and u_i is the corresponding velocity component. n_j is a unit normal vector on S, and τ_{ij} indicates the effective viscous stress. In addition, b_i indicates the body force. Spatial discretization is carried out using the GAMMA scheme for the convective term and the central difference scheme for the diffusive term based on the collocated grid system. The first-order implicit Euler method is used in temporal discretization. The SIMPLE method with several correction steps is applied to couple the pressure and velocity field. It is well-known that checker-board instability can occur in the collocated arrangement of fluid variables. In order to remedy this problem, the mo-

mentum interpolation method suggested by Rhie and Chow [10] is utilized with additional correction by Choi [11]. Final algebraic linear systems are solved by the Bi-CGSTAB algorithm.

Two-phase fluids are treated as a single continuum while implicitly capturing the interface. In the physical domain, the fluid density and viscosity are changed according to the volume fraction α.

$$\rho = \rho_1\alpha + \rho_2(1-\alpha) \quad (13)$$

$$\mu = \mu_1\alpha + \mu_2(1-\alpha) \quad (14)$$

In the present VOF method, an additional scalar convection equation for the volume fraction should be solved simultaneously with the Navier-Stoke equation.

$$\frac{\partial}{\partial t}\int_\Omega \alpha d\Omega + \int_S \alpha u_j n_j dS = 0 \quad (15)$$

Ubbink and Issa [4] suggested a new high resolution method (CICSAM) for the accurate capturing of fluid interfaces on the meshes of an arbitrary topology. In this scheme, two high resolution discretization schemes, the convection boundedness criteria (CBC) and the ultimate quickest (UQ), are appropriately combined to ensure the preservation of the sharpness and the shape of the interface while retaining the boundedness of the field.

$$\alpha_f = \beta_f \alpha_{f,CBC} + (1-\beta_f)\alpha_{f,UQ} \quad (16)$$

where β_f is a weighting factor which takes into account the slope of the free surface relative to the direction of motion. More details about the CICSAM scheme can be found in Ubbink and Issa [4].

4. Results and discussion

4.1 Dam-breaking problem with an obstacle

The dam-breaking problem is a typical benchmarking problem used to validate complex flow patterns such as fragmentation, overturning and reunification. The experiment for the present computational model has been carried out at the Maritime Research Institute Netherlands (MARIN). A large tank of 3.22×1.00×1.00m is used with an open roof. Inside the tank, a small box has been placed on the bottom. The initial conditions and measuring locations are given in Fig.2, and the detail experiment conditions can be found in Kleefsman et al. [12].

Free-surface snapshots taken directly before and after the water hits the bottom box are compared with the experimental observation in Fig. 3. The comparison shows that reasonable results can be obtained using the present numerical methods in free-surface shapes before the impact. Some differences can be found between the two numerical results and the experiment after the impact. The detailed water splash around the obstacle cannot be simulated in computations due to the mesh resolution and numerical diffusion. However, the global flow motions are very similar.

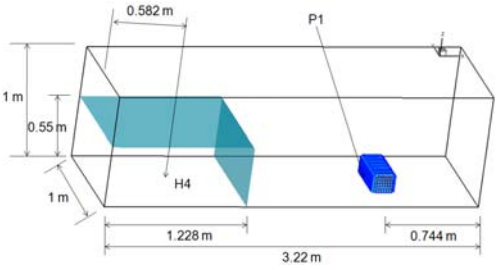

Fig. 2. Schematic view of dam-breaking problem

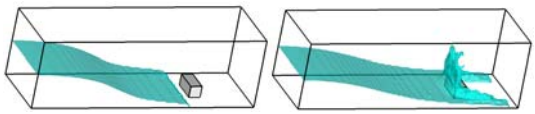

<CIP, $t\sqrt{g/h_0}=1.69$ > <CIP, $t\sqrt{g/h_0}=2.53$ >

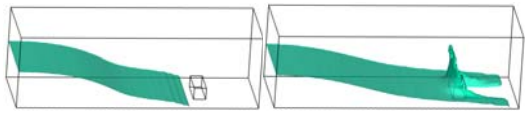

<FV, $t\sqrt{g/h_0}=1.69$ > <FV, $t\sqrt{g/h_0}=2.53$ >

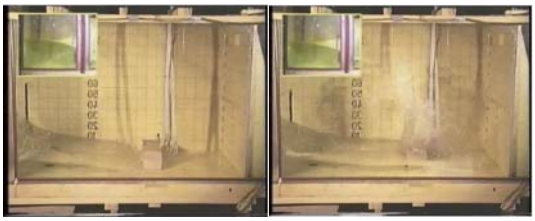

<Exp., $t\sqrt{g/h_0}=1.69$ > <Exp., $t\sqrt{g/h_0}=2.37$ >

Fig. 3. Comparisons of snapshots for dam-breaking problem

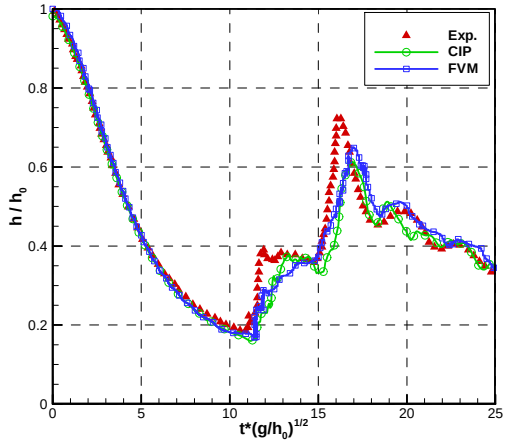

Fig. 4. Comparison of water heights measured at *H*4

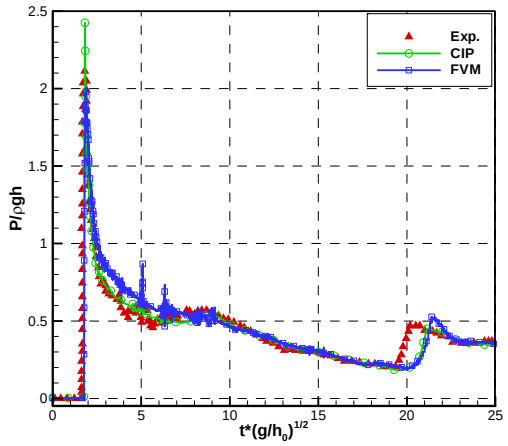

Fig. 5. Comparison of pressure time histories measured at *P*1

Fig. 4 shows the total water height measured at the initial water column (*H*4). The figure shows almost the same results before the water hits the left wall ($t\sqrt{g/h_0}=11.5$). This means that the decreasing rate of water height is similar to the computations and the experiment, while the reversing wave situations differ with each other. When the impact occurs with the bottom obstacle, there are a large number of water splashes which are difficult to simulate by using conventional computation methods and moderate mesh resolution. Thus, during the impact, some physical quantities are lost and this affects the flow characteristics such as wave speed and free-surface shape.

In Fig. 5, the local pressure (*P*1) measured at the front of the box placed in the tank bottom is compared with the experiment data. The local pressure also differs between the computational results and experiment data near $t\sqrt{g/h_0}=20$. At this point, the wave return again to the box after it hit the left wall. Since detail conditions such as bottom roughness and turbulence modeling differ with the experiment, some discrepancy between the computations and the experiment result is inevitable.

4.2 Diffraction problem for truncated cylinder

The accurate predictions of wave run-up and wave-induced load on a circular cylinder are important for the design of offshore structures, and the degree of accuracy of the predictions is a parameter for estimating the ability of a numerical method. In this study, a truncated vertical circular cylinder with a diameter of 16m and a draft of 24m is considered. This model has been experimentally investigated by Sung et al. [13]. The computational domain is a rectangular wave tank with a length of 5λ, a depth of 20a, and a half-width of 9a, as shown in Fig. 6.

Wave elevations measured at two locations of the weather side (*E*1) and lee side (*E*5) are compared in Fig. 7. In the case of *E*1, the CIP-based method gives a similar result as the experiment data, while the FV-based method result slightly differs in both amplitude and phase. On the other hand, the CIP-based method shows a smaller wave elevation at *E*5, while the FV-based method shows almost the same maximum wave height. Since the body boundary condition does not satisfy exact position of the circular cylinder in the CIP-based method, this shows that some amount of fluid remained at the cylinder surface. Thus, this may result in a smaller wave height in the wake region.

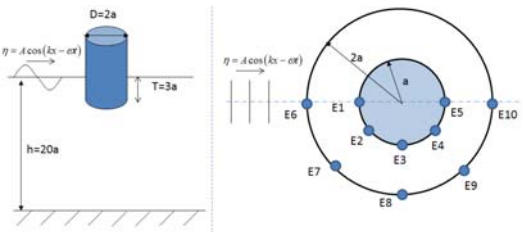

Fig. 6. Schematic view of diffraction problem for truncated cylinder and measuring locations of wave height

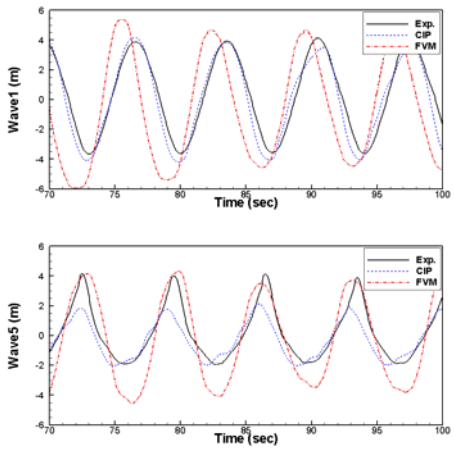

Fig. 7 Comparisons of wave elevations measured at *E*1 (upper) and *E*5 (lower)

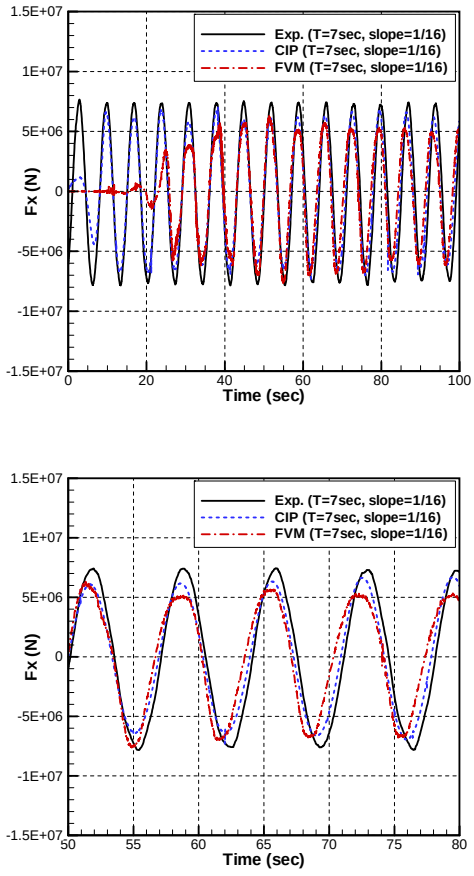

Fig. 8 Comparisons of surge force signals (upper), enlarged between 50~80 sec (lower)

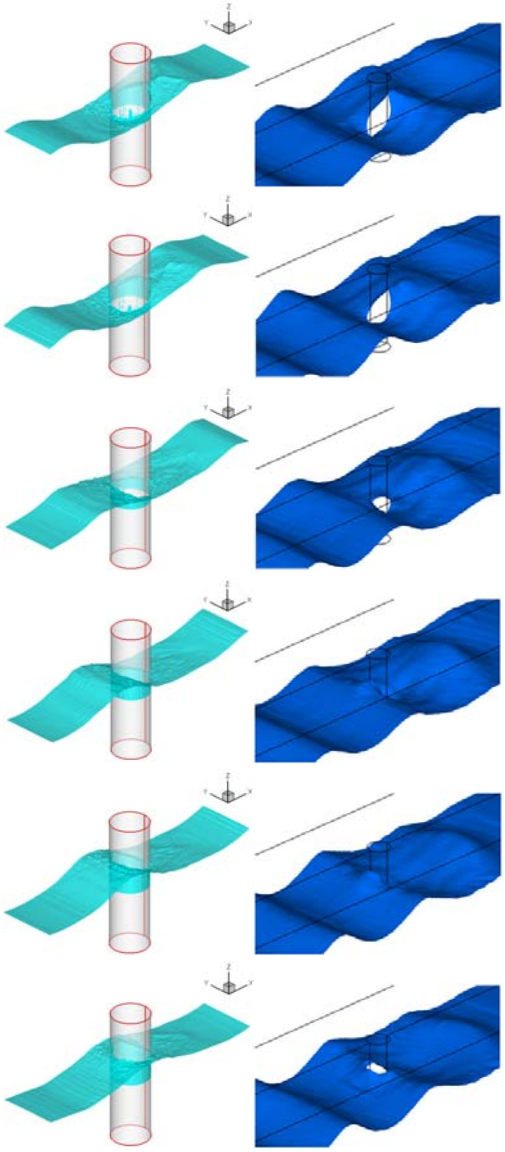

Fig. 9 Snapshots of diffraction problem for truncated cylinder

In Fig. 8, the time-history of the surge force is compared with the experimental data. The CIP-based method provides the computational result to the experimental data closer than the FVM result for force magnitude and phase. Since computation using a staggered Cartesian grid ensures a more accurate incident wave, the diffraction force is also more accurate in the CIP-based method than in the FV-based method results. However, both methods give a slightly smaller surge force than the experimental data.

Sequential snapshots for the case in which the wave period is 7sec and wave slope is 1/16 are compared during one period in Fig. 9. The global wave patterns are similar between the CIP-based and FV-based methods, but the detailed free-surface profiles around the body show some differences. The CIP result shows "stair-stepping" behavior because the volume fraction is interpolated by a tangent hyperbolic function in the THINC method, while the FV-based method provides a smooth free-surface shape.

5. Conclusions

In the present study, two different methods, the CIP-based and FV-based methods, are applied to solve three-dimensional wave-body interaction problems including the dam-breaking problem with an obstacle and the diffraction problem for a truncated cylinder. Based on the present study, the following conclusions can be made:

- In solving the dam-breaking problem, both methods provide similar results to the experiment. When the fluid flow becomes very violent, the numerical results slightly differ from the experimental data due to water splash, bottom roughness, and turbulence modeling etc.
- The THINC method gives "stair-step" behavior in the free-surface shape, while the CICSAM method gives a smoother wave profile. However, both methods provide a reasonable free-surface motion.
- In solving the diffraction problem for the truncated cylinder, the CIP-based method provides computational results that are closer to the experimental data than the FV-based method in the wave-elevation at the cylinder front and surge force. However, in the wake region, the FV-based method gives a better wave-elevation result than the CIP-based method. A more solid conclusion for this finding can be made after more systematic computation and comparison.

Acknowledgements

This study has been supported by The LRET-funded Research Center at Seoul National University (LRETC) and also by the principal R&D program of KORDI: "Performance Evaluation Technologies of Offshore Operability for Transport and Installation of Offshore Structures" granted by the Korea Research Council of Fundamental Science and Technology. Their support is greatly appreciated. Also, the administrative support by ERI and RIMSE should be credited.

References

[1] C. Yang and R. Löehner, *On the Modeling of Highly Nonlinear Wave-Body Interactions*, Proc. 16th Int. Offshore and Polar Eng. Conf., San Francisco, USA, ISOPE, (2006) 256-263.

[2] C. Hu, M. Kashiwagi, M. Sueyoshi and I. Nakagiri, *Numerical Simulation of Strongly Nonlinear Wave-Ship Interaction by CIP/Cartesian Grid Method*, Proc. 18th Int. Offshore and Polar Eng. Conf., Vancouver, Canada, ISOPE, (2008) 143-147.

[3] C. Monroy, G. Ducrozet, P. Roux, L. Gentaz, P. Ferrant and B. Alessandrini, *RANS Simulations of Ship Motions in Regular and Irregular Head Seas using the SWENSE Method*, Proc. 19th Int. Offshore and Polar Eng. Conf., Osaka, Japan, ISOPE, (2009) 458-465.

[4] O. Ubbink and R. I. Issa, *A Method for Capturing Sharp Fluid Interfaces on Arbitrary Meshes*, J. of Computational Physics, 153 (1999) 26-50.

[5] F. Xiao, Y. Honma and T. Kono, *A Simple Algebraic Interface Capturing Scheme using Hyperbolic Tangent Function*, Int. J. for Numerical Methods in Fluids, 48 (2005) 1023-1040.

[6] H. Takewaki and T. Yabe, *The Cubic-Interpolated Pseudo Particle (CIP) Method Application to Nonlinear and Multi-Dimensional Hyperbolic Equations*, J. of Computational Physics, 70 (1987) 355-372.

[7] T. Yabe, *A Universal Cubic Interpolation Solver for Compressible and Incompressible Fluids*, Shock Waves, 1 (1991) 187-195.

[8] F. Xiao, T. Yabe, G. Nizam and T. Ito, *Constructing a Multi-Dimensional Oscillation Preventing Scheme for Advection Equation by a Rational Function*, Computer Physics Communications, 94 (1996) 103-118.

[9] J. H. Ferziger and M. Peric, *Computational Methods for Fluid Dynamics*, Springer-Verlag, Heidelberg, (2002).

[10]C. M. Rhie and W. L. Chow, *Numerical Study of the Turbulent Flow Past an Airfoil with Trailing Edge Separation*, AIAA J., 21 (1983) 1525-1532.

[11]S. K. Choi, *Note on the Use of Momentum Interpolation Method for Unsteady Flow*, Numerical Heat Transfer A, 36 (1999) 545-550.

[12]K. M. T. Kleefsman, G. Fekken, A. E. P. Veldman, B. Iwanowski and B. Buchner, *A Volume-of-Fluid based Simulation Method for Wave Impact Problems*, J. Computational Physics, 206 (2005) 363-393.

[13]H. G. Sung, Y. S. Kim, B. W. Nam and S. Y. Hong, *QExperimental Investigation of Wave Loads on a Truncated Vertical Circular Cylinder*, Proc. Korean Society of Ocean Enginerrs (in Korean), (2007).